



ISME

R. Poultangari *
MSc

A. Bahtui †
Post-Graduate Student

M.R. Eslami ‡
Professor

Thermoelastic Analysis in Thick FGM Cylinders with Extended Profile

An exact solution is obtained for an axisymmetric steady-state thermo-mechanical stresses in a thick functionally graded cylinder. The material properties are graded along the radial direction according to an exponential function of radial direction with three constants. The advantage of the proposed model, compared to the models with two constants such as the linear, power law, and exponential models with two constants, is that it satisfies the material boundary conditions at the inside and outside radiuses, leaving one more constant to be selected to produce different types of material variation profiles along the cylinder radius. Utilizing the assumed exponential model, the analytical solution of the problem, using the generalized Bessel function and the Lagrange method, is obtained employing the energy and Navier equations.

Key words: *exponential; FGM; model; symmetric; thermal stresses; thick; cylinder*

1 Introduction

The one-dimensional steady thermal stresses in a functionally graded circular hollow cylinder and hollow sphere using the perturbation method is given by Obata and Noda [1]. By introducing the theory of laminated composites, Ootao et al. [2] presented the theoretical analysis of a three-dimensional thermal stress problem for a nonhomogeneous hollow circular cylinder due to a moving heat source in the axial direction under transient state. Tanigawa et al. [3] solved the thermal stresses for a semi-infinite body with the assumption that the nonhomogeneous material properties are power functions of the thickness direction z . Jabbari et al. [4,5] derived the analytical solutions for the one and two-dimensional steady-state thermoelastic problems of the functionally graded circular hollow cylinder, where the material properties are expressed by power functions of radius. Lutz and Zimmerman [6,7] presented the analytical solution for thermal stresses in spheres and cylinders made of functionally graded materials (FGMs). They considered thick spheres and cylinders under radial thermal loads, where radially graded materials with linear composition of the constituent materials were considered. Shao et al. [8] presented the analytical solutions of the stress fields in functionally graded cylindrical panel with

* MSc, Department of Mechanical Engineering, Islamic Azad University, Dezfoul Branch, Iran, poultangari@iaud.ac.ir

† GPost-Graduate Student, System and Design Department, Brunel University, Middlesex, UB8 3PH, UK, Ali.Bahtui@Brunel.ac.uk

‡ Professor and Fellow of the Academy of Sciences, ME Dept., Amirkabir University of Technology, Tehran, Iran

finite length subjected to thermomechanical loading. In this paper, they employed the power law FGM variation model to illustrate the variations of properties along the radial direction of the panel. Yee and Moon [9] obtained a closed-form solution for the transient thermal stresses of an orthotropic hollow cylinder subjected to an asymmetric temperature distribution. Tarn [10] examined the stress singularity in an elastic cylinder of cylindrically anisotropic materials in the context of generalized plain strain and generalized torsion condition. Eslami et al. [11] and Poultangari et al. [12] derived an exact solution for the one and two-dimensional steady-state thermal and mechanical stresses in a hollow thick sphere made of functionally graded material. In these papers, they used the power law FGM variation to describe the material properties along the radial direction of the sphere. You et al. [13] presented the elastic analysis of internally pressurized thick wall spherical pressure vessels of FGM. Tutuncu [14] solved the stress problem in a thick wall FGM cylinder with inner pressure. In both Refs. [13] and [14] the authors used the same exponential FGM model for the variation of properties with radial direction. This model, similar to the power law model, has two variables to describe the material properties in the radial direction. Therefore, for fixed inner and outer material properties, a single material property profile along the thickness is generated.

The analytical solution of the structures made of functionally graded materials and discussed in the proceeding paragraph have, in general, employed FGM variation models for the material properties with two constants. Using the two constants constitutive law for the FGM thick cylinders or spheres results into a fixed FGM profile along the radial direction when the material boundary conditions at the inside and outside surfaces are satisfied. For more general FGM models, such as Reddy [15] and Tanigawa [3] models, which satisfy the given material boundary conditions for more than one profile, there are no exact solutions in the literature.

In this study, an FG hollow circular cylinder with a constitutive model containing three independent constants is considered. The temperature distribution is assumed to be axisymmetric and function of r . The material properties of the cylinder are assumed to be expressed by exponential functions of the radial direction with three arbitrary constants. The solution for the energy equation leads to the generalized Bessel function [16]. The homogeneous part of the Navier equation also leads to the generalized Bessel function. The method of variation of parameters is used to solve the particular solution of the Navier equation.

2 Analysis of Energy Equation

The steady-state temperature distribution in an FGM circular hollow cylinder is governed by the following energy equation [17]

$$\frac{1}{r}(rk(r)T'(r))' = 0 \quad (1)$$

where $T(r)$ is the temperature distribution and $k = k(r)$ is the thermal conduction coefficient and $(')$ denotes differentiation with respect to r . The Robin-type boundary conditions are considered as

$$\begin{aligned} C_{11}T'(a) + C_{12}T(a) &= f_1 \\ C_{21}T'(b) + C_{22}T(b) &= f_2 \end{aligned} \quad (2)$$

where C_{ij} are the thermal boundary condition coefficients and a and b are the inside and outside radiuses, respectively. Functions f_1 and f_2 are known boundary conditions on the inside and

outside radii. The thermal conductivity $k(r)$ may be assumed to be expressed by the exponential function of r as

$$P_3(r) = k(r) = \frac{\beta_3}{r^{\gamma_3}} e^{\frac{\lambda_3}{\theta_3} r^{\theta_3}} \quad (3)$$

where β_3 , λ_3 , θ_3 , and γ_3 are unknown constants to be found. In order to satisfy the inner and outer material boundary conditions, the constants β_3 and λ_3 are obtained as

$$\begin{aligned} \lambda_i &= \frac{\theta_i}{b^{\theta_i} - a^{\theta_i}} \ln \left[\frac{P_i(b)}{P_i(a)} \left(\frac{b}{a} \right)^{\gamma_i} \right] \\ \beta_i &= P_i(a) a^{\gamma_i} e^{-\frac{\lambda_i}{\theta_i} a^{\theta_i}} \quad i = 3. \end{aligned} \quad (4)$$

Since θ_3 is further restricted, the choice of γ_3 produces different material profile variations between the inside and outside surfaces. Substituting Eq. (3) into the energy equation yields

$$r^2 T''(r) + r [(1 - \gamma_3) + \lambda_3 r^{\theta_3}] T' = 0 \quad (5)$$

For $\theta_3 = \gamma_3$ (a restriction for θ_3), Eq. (5) becomes the generalized Bessel equation (see Appendices I and II), which has a general solution as

$$T(r) = r^{\alpha_3} e^{-\zeta_3 r^{\theta_3}} \left[AI_{\frac{1}{2}}(\zeta_3 r^{\theta_3}) + BI_{-\frac{1}{2}}(\zeta_3 r^{\theta_3}) \right] = \bar{A} + \bar{B} e^{-2\zeta_3 r^{\theta_3}} \quad (6)$$

where A and B , or \bar{A} and \bar{B} , are unknown constants to be found from the thermal boundary conditions (2) and

$$\begin{aligned} \alpha_3 &= \frac{\theta_3}{2} \\ \zeta_3 &= \frac{\lambda_3}{2\theta_3}. \end{aligned} \quad (7)$$

Here, $I_{\pm\frac{1}{2}}$ is the modified Bessel function of the first kind and the $\pm\frac{1}{2}$ th. order.

3 Thermal Stress Analysis

The governing strain-displacement relations are

$$\epsilon_{rr} = u', \quad \epsilon_{\theta\theta} = \frac{u}{r} \quad (8)$$

where u is the displacement component along the radial direction. The stress-strain relations for the plane-strain condition are

$$\begin{aligned} \sigma_{rr} &= \frac{E}{(1 + \nu)(1 - 2\nu)} [(1 - \nu)\epsilon_{rr} + \nu\epsilon_{\theta\theta} - (1 + \nu)\alpha T] \\ \sigma_{\theta\theta} &= \frac{E}{(1 + \nu)(1 - 2\nu)} [\nu\epsilon_{rr} + (1 - \nu)\epsilon_{\theta\theta} - (1 + \nu)\alpha T] \end{aligned}$$

$$\sigma_{zz} = \frac{E}{(1+\nu)(1-2\nu)} [\nu(\epsilon_{rr} + \epsilon_{\theta\theta}) - (1+\nu)\alpha T] \quad (9)$$

where α is the coefficient of thermal expansion, E is the modulus of elasticity, ν is the Poisson's ratio, and σ_{ii} ($i = r, \theta, z$) are the normal stresses. The one-dimensional static equilibrium equation is

$$\sigma'_{rr} + \frac{1}{r}(\sigma_{rr} - \sigma_{\theta\theta}) = 0 \quad (10)$$

The modulus of elasticity and the coefficient of thermal expansion are described with an exponential functions of the radial direction as

$$P_1(r) = E(r) = \frac{\beta_1}{r^{\gamma_1}} e^{\frac{\lambda_1}{\theta_1} r^{\theta_1}}, \quad P_2(r) = \alpha(r) = \frac{\beta_2}{r^{\gamma_2}} e^{\frac{\lambda_2}{\theta_2} r^{\theta_2}} \quad (11)$$

where β_i and λ_i ($i = 1, 2$) are obtained from Eq. (4). Substituting $i = 1, 2$, θ_1 and θ_2 are further restricted, and γ_1 and γ_2 are free to be changed to provide different material property profiles along the radius. We may further assume that the Poisson's ratio is constant. Using Eqs. (8) through (11), the Navier equation in terms of the displacement becomes

$$r^2 u''(r) + (\lambda_1 r^{\theta_1} - \gamma_1 + 1) r u'(r) + \left[\frac{\nu}{1-\nu} \lambda_1 r^{\theta_1} - \frac{\nu}{1-\nu} \gamma_1 - 1 \right] u(r) = \beta_2 e^{\frac{\lambda_2}{\theta_2} r^{\theta_2} - \gamma_2 \ln r} \frac{1+\nu}{1-\nu} r [(\lambda_1 r^{\theta_1} + \lambda_2 r^{\theta_2} - (\gamma_1 + \gamma_2)) T(r) + r T'(r)]. \quad (12)$$

4 Solution of the Navier Equation

The homogeneous part of the Navier equation (12) is

$$r^2 u''(r) + (\lambda_1 r^{\theta_1} - \gamma_1 + 1) r u'(r) + \left[\frac{\nu}{1-\nu} \lambda_1 r^{\theta_1} - \frac{\nu}{1-\nu} \gamma_1 - 1 \right] u(r) = 0 \quad (13)$$

Substituting $\theta_i = \gamma_i + \frac{2\nu}{1-\nu}$ ($i = 1, 2$) into Eq. (13), leads to the generalized Bessel differential equation (see Appendices I and II), which has a general solution as

$$u_g(r) = r^{\alpha_1} e^{-\zeta_1 r^{\theta_1}} [C I_p(\zeta_1 r^{\theta_1}) + D I_{-p}(\zeta_1 r^{\theta_1})] \quad (14)$$

where

$$\begin{aligned} p &= \frac{1}{\theta_1} \sqrt{\left(\frac{\gamma_1}{2}\right)^2 + \frac{\nu\gamma_1}{1-\nu} + 1} \\ \alpha_1 &= \frac{1}{2}\theta_1 - \frac{\nu}{1-\nu} \\ \zeta_i &= \frac{\lambda_i}{2\theta_i} \quad (i = 1, 2) \end{aligned} \quad (15)$$

and C and D are unknown constants to be found from the boundary conditions. Let χ_1 to χ_4 be known boundary conditions on the inner and outer radii, respectively. Therefore, the stress or displacement boundary conditions are

$$\begin{aligned}
u(a) &= \chi_1 \\
u(b) &= \chi_2 \\
\sigma_{rr}(a) &= \chi_3 \\
\sigma_{rr}(b) &= \chi_4
\end{aligned} \tag{16}$$

The constants C and D are obtained solving a system of two algebraic equations, selected arbitrarily from the list given by Eqs. (16). For thermal stresses, any combination of the kinematical or stress boundary conditions given by Eqs. (16) is permissible. For the cylinders under pure mechanical stresses, either displacement or stress boundary conditions may be selected from the list of Eqs. (16).

The particular solution $u_p(r)$ is obtained using the method of variation of parameters. Equation (12) may be written in the form of variation of parameters formula as

$$u_p''(r) + f(r)u_p'(r) + g(r)u_p(r) = h(r) \tag{17}$$

where

$$\begin{aligned}
f(r) &= \frac{1}{r} (\lambda_1 r^{\theta_1} - \gamma_1 + 1) \\
g(r) &= \frac{1}{r^2} \left[\frac{\nu}{1-\nu} (\lambda_1 r^{\theta_1} - \gamma_1) - 1 \right] \\
h(r) &= \beta_2 \frac{1+\nu}{1-\nu} r^{\alpha_3-1} e^{\left(\frac{\lambda_2}{\theta_2} r^{\theta_2} - \gamma_2 \ln r - \zeta_3 r^{\theta_3}\right)} \times \\
&\left\{ \left[(\lambda_1 r^{\theta_1} - \gamma_1) + (\lambda_2 r^{\theta_2} - \gamma_2) - \frac{1}{2} (\lambda_3 r^{\theta_3} - \gamma_3) \right] \left[AI_{\frac{1}{2}}(\zeta_3 r^{\theta_3}) + BI_{-\frac{1}{2}}(\zeta_3 r^{\theta_3}) \right] + \right. \\
&\left. r \left[AI'_{\frac{1}{2}}(\zeta_3 r^{\theta_3}) + BI'_{-\frac{1}{2}}(\zeta_3 r^{\theta_3}) \right] \right\}
\end{aligned} \tag{18}$$

Let the general solution obtained in Eq. (17) be divided into two parts $u_{g1}(r)$ and $u_{g2}(r)$ as

$$\begin{aligned}
u_{g1}(r) &= r^{\alpha_1} e^{-\zeta_1 r^{\theta_1}} I_p(\zeta_1 r^{\theta_1}) \\
u_{g2}(r) &= r^{\alpha_1} e^{-\zeta_1 r^{\theta_1}} I_{-p}(\zeta_1 r^{\theta_1})
\end{aligned} \tag{19}$$

Therefore, the particular solution $u_p(r)$, according to the method of variation of parameters, becomes

$$u_p(r) = -u_{g1}(r) \int_a^r \frac{u_{g2}(\bar{r})}{w(\bar{r})} h(\bar{r}) d\bar{r} + u_{g2}(r) \int_a^r \frac{u_{g1}(\bar{r})}{w(\bar{r})} h(\bar{r}) d\bar{r} \tag{20}$$

where $w(r)$ is the Wronskian determinant of $u_{g1}(r)$ and $u_{g2}(r)$ as given by

$$w(r) = u_{g1}(r)u_{g2}'(r) - u_{g2}(r)u_{g1}'(r) \tag{21}$$

$$u_{g1}'(r) = \left[(\alpha_1 - \zeta_1 \theta_1 r^{\theta_1}) I_p(\zeta_1 r^{\theta_1}) + r I_p'(\zeta_1 r^{\theta_1}) \right] r^{\alpha_1-1} e^{-\zeta_1 r^{\theta_1}}$$

$$u'_{g_2}(r) = [(\alpha_1 - \zeta_1 \theta_1 r^{\theta_1}) I_{-p}(\zeta_1 r^{\theta_1}) + r I'_{-p}(\zeta_1 r^{\theta_1})] r^{\alpha_1-1} e^{-\zeta_1 r^{\theta_1}} \quad (22)$$

where $I'_{\pm p}(\zeta_1 r^{\theta_1})$ is the derivative of $I_{\pm p}(\zeta_1 r^{\theta_1})$ with respect to r as

$$I'_{\pm p}(\zeta_1 r^{\theta_1}) = \zeta_1 \theta_1 r^{\theta_1-1} I_{\pm p+1}(\zeta_1 r^{\theta_1}) \pm \frac{p\theta_1}{r} I_{\pm p}(\zeta_1 r^{\theta_1}) \quad (23)$$

The complete solution for $u(r)$ is the sum of the general and particular solutions. Therefore, using Eqs. (14) and (20) yields

$$u(r) = \left[C - \int_a^r Q_2(\bar{r}) d\bar{r} \right] u_{g_1}(r) + \left[D + \int_a^r Q_1(\bar{r}) d\bar{r} \right] u_{g_2}(r) \quad (24)$$

where

$$\begin{aligned} Q_1(r) &= \frac{u_{g_1}(r)}{w(r)} h(r) \\ Q_2(r) &= \frac{u_{g_2}(r)}{w(r)} h(r) \end{aligned} \quad (25)$$

The strains and stresses are obtained by substituting Eqs. (24) and (25) into Eqs. (8) and (9), which yield

$$\begin{aligned} \epsilon_{rr}(r) &= r^{\alpha_1-1} e^{-\zeta_1 r^{\theta_1}} \left\{ \left[C - \int_a^r Q_2(\bar{r}) d\bar{r} \right] [(\alpha_1 - \zeta_1 \theta_1 r^{\theta_1} + p\theta_1) I_p(\zeta_1 r^{\theta_1}) + \zeta_1 \theta_1 r^{\theta_1} I_{p+1}(\zeta_1 r^{\theta_1})] + \right. \\ &\quad \left. \left[D + \int_a^r Q_1(\bar{r}) d\bar{r} \right] [(\alpha_1 - \zeta_1 \theta_1 r^{\theta_1} - p\theta_1) I_{-p}(\zeta_1 r^{\theta_1}) + \zeta_1 \theta_1 r^{\theta_1} I_{-p+1}(\zeta_1 r^{\theta_1})] - \right. \\ &\quad \left. Q_2(r) r I_p(\zeta_1 r^{\theta_1}) + Q_1(r) r I_{-p}(\zeta_1 r^{\theta_1}) \right\} \end{aligned} \quad (26)$$

$$\epsilon_{\theta\theta}(r) = r^{\alpha_1-1} e^{-\zeta_1 r^{\theta_1}} \left\{ \left[C - \int_a^r Q_2(\bar{r}) d\bar{r} \right] I_p(\zeta_1 r^{\theta_1}) + \left[D + \int_a^r Q_1(\bar{r}) d\bar{r} \right] I_{-p}(\zeta_1 r^{\theta_1}) \right\} \quad (27)$$

$$\begin{aligned} \begin{bmatrix} \sigma_{rr} \\ \sigma_{\theta\theta} \\ \sigma_{zz} \end{bmatrix} &= \left\{ \left[C - \int_a^r Q_2(\bar{r}) d\bar{r} \right] [(\alpha_1 - \zeta_1 \theta_1 r^{\theta_1} + p\theta_1) I_p(\zeta_1 r^{\theta_1}) + \zeta_1 \theta_1 r^{\theta_1} I_{p+1}(\zeta_1 r^{\theta_1})] + \right. \\ &\quad \left. \left[D + \int_a^r Q_1(\bar{r}) d\bar{r} \right] [(\alpha_1 - \zeta_1 \theta_1 r^{\theta_1} - p\theta_1) I_{-p}(\zeta_1 r^{\theta_1}) + \zeta_1 \theta_1 r^{\theta_1} I_{-p+1}(\zeta_1 r^{\theta_1})] - \right. \\ &\quad \left. Q_2(r) r I_p(\zeta_1 r^{\theta_1}) + Q_1(r) r I_{-p}(\zeta_1 r^{\theta_1}) \right\} \begin{bmatrix} 1 - \nu \\ \nu \\ \nu \end{bmatrix} + \left\{ \left[C - \int_a^r Q_2(\bar{r}) d\bar{r} \right] I_p(\zeta_1 r^{\theta_1}) + \right. \\ &\quad \left. \left[D + \int_a^r Q_1(\bar{r}) d\bar{r} \right] I_{-p}(\zeta_1 r^{\theta_1}) \right\} \begin{bmatrix} \nu \\ 1 - \nu \\ \nu \end{bmatrix} \left. \right\} \frac{\beta_1}{(1 + \nu)(1 - 2\nu)} r^{-\alpha_1-1} e^{\zeta_1 r^{\theta_1}} \\ &\quad - \frac{\beta_1 \beta_2}{1 - 2\nu} \frac{e^{(2\zeta_1 r^{\theta_1} + 2\zeta_2 r^{\theta_2} - \zeta_3 r^{\theta_3})}}{r^{(2\alpha_1 + 2\alpha_2 - \alpha_3)}} \left[AI_{\frac{1}{2}}(\zeta_3 r^{\theta_3}) + BI_{-\frac{1}{2}}(\zeta_3 r^{\theta_3}) \right] \begin{bmatrix} 1 \\ 1 \\ 1 \end{bmatrix} \end{aligned} \quad (28)$$

The values of C and D are evaluated from two mechanical boundary conditions, which are arbitrarily (physically meaningful) selected from Eqs. (16).

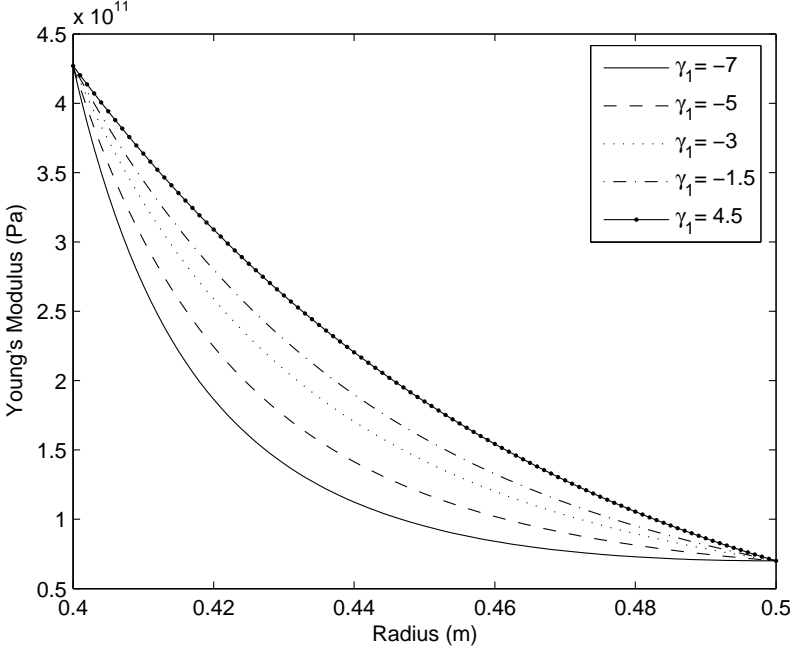


Figure 1 Young's modulus along the radius of a functionally graded cylinder.

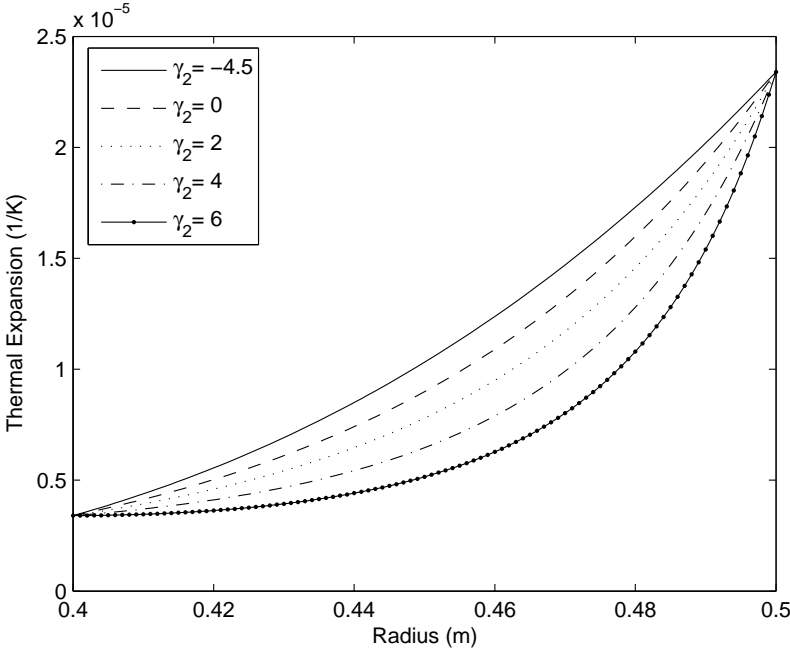


Figure 2 Coefficient of thermal expansion along the radius of a functionally graded cylinder.

Table 1 Material properties of a typical FGM

Metal (outer):	= Ceramics (inner):
$E = 70(GPa)$	$E = 427(GPa)$
$\nu = 0.3$	$\nu = 0.3$
$\alpha = 23.4 \times 10^{-6}(1/K)$	$\alpha = 3.4 \times 10^{-6}(1/K)$
$k = 233(W/mK)$	$k = 65(W/mK)$

Table 2 Definition of cases

Cases	γ_1	γ_2	γ_3
Case 1	-7	-4.5	-3
Case 2	-5	0	2
Case 3	-3	2	4
Case 4	-1.5	4	5.5
Case 5	4.5	6	6.5

5 Results

Consider a thick hollow cylinder of inner radius $a = 40 \text{ cm}$ and outer radius $b = 50 \text{ cm}$. The material properties of the functionally graded cylinder are given in Table (1). The variation of modulus of elasticity, coefficient of thermal expansion, and heat conduction coefficient along the radial direction are plotted in Figs. (1) through (3). These figures are plotted for different values of γ .

To validate the results of this analysis, we may reduce the problem to that of isotropic thick cylinder by proper selection of numerical values for γ 's. Selection of $\gamma_1 = -1$, $\gamma_2 = 0$, and $\gamma_3 = 0.2$ produce a thick cylinder with isotropic material properties, where its behaviour under thermal or mechanical load is known. This condition is checked with the formulations of this paper, where exact results are obtained. Therefore, using identical material properties, boundary conditions, and the same geometry as given and defined by references [4,17], identical curves for the displacement and stress distributions, as shown in Figs. (4) and (5), are obtained.

The discussion of thermal stresses in the FGM thick cylinders with different material profiles are defined in a set of different cases, as shown in Table (2). The curve associated with the largest negative value of γ represents more ceramic rich, and that of largest positive value of γ represents more metal rich FGM. Various FGM variation profiles across the thickness is produced by choosing arbitrary values for γ_1 , γ_2 , and γ_3 . These constants (γ_1 , γ_2 , γ_3) provide various material property profiles for the modulus of elasticity, coefficient of thermal expansion, and the coefficient of the thermal conductivity, respectively. Therefore, five arbitrary material variation profiles are defined in five different sets such that in each set a fixed combination for γ is defined. These sets are defined in five cases, where case 1 is the most metal-rich, and case 5 is the most ceramic-rich functionally graded material. The numerical values for γ 's for the cases 1 through 5 are given in Table (2). Note that the FGM profiles for each value of γ 's are shown in Figs. (1) through (3).

Consider a thick cylinder with traction-free boundaries at the inner and outer surfaces. The temperature for the inner and outer surfaces are assumed to be $T(a) = 50K$ and $T(b) = 0K$. In Fig. (6) the temperature distribution along the radial direction is presented. This figure shows that the magnitude of temperatures are decreased in metal rich FGMs, where γ has the largest positive magnitude. The resulting thermoelastic radial displacement due to the applied temperature variations is presented in Fig. (7). According to this figure, by increasing the

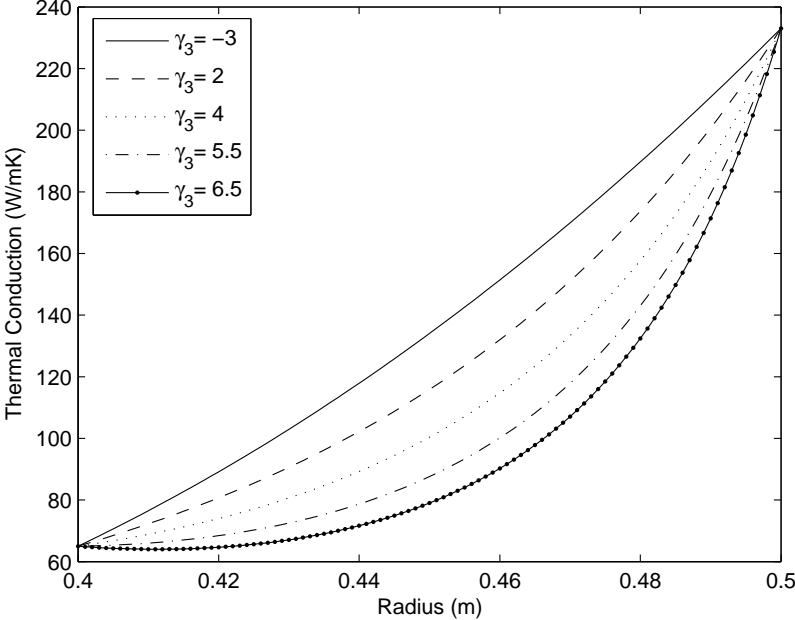


Figure 3 Coefficient of thermal conduction along the radius of a functionally graded cylinder.

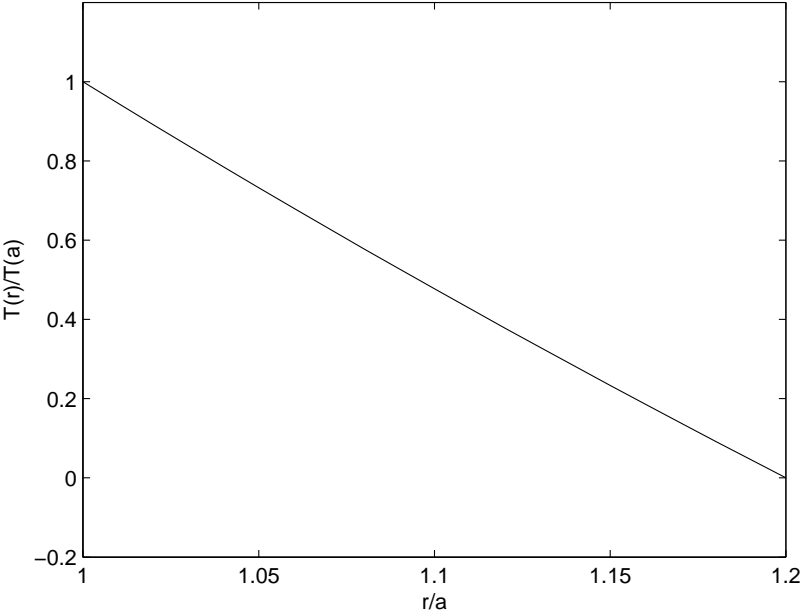


Figure 4 Temperature distribution in a homogeneous cylinder (validation).

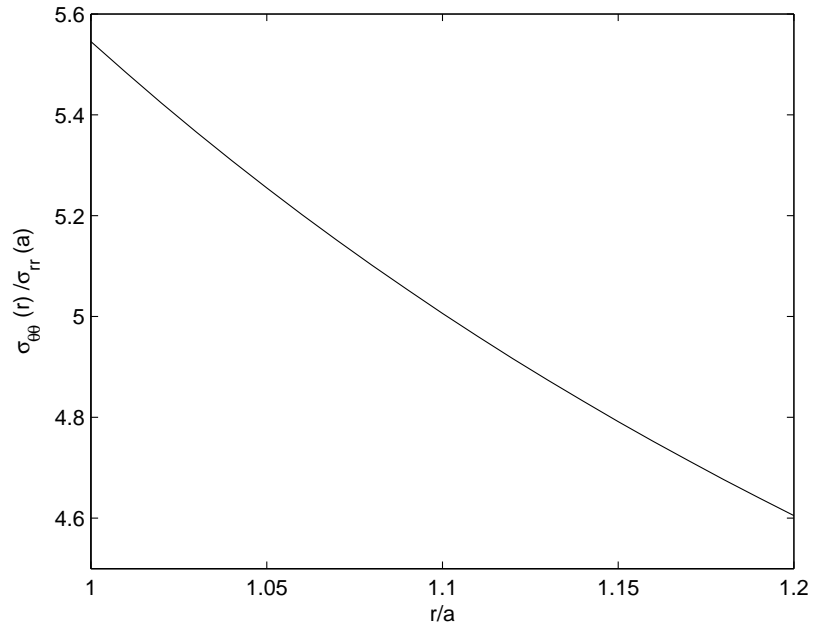


Figure 5 Hoop thermo-mechanical stress in a homogeneous cylinder (validation).

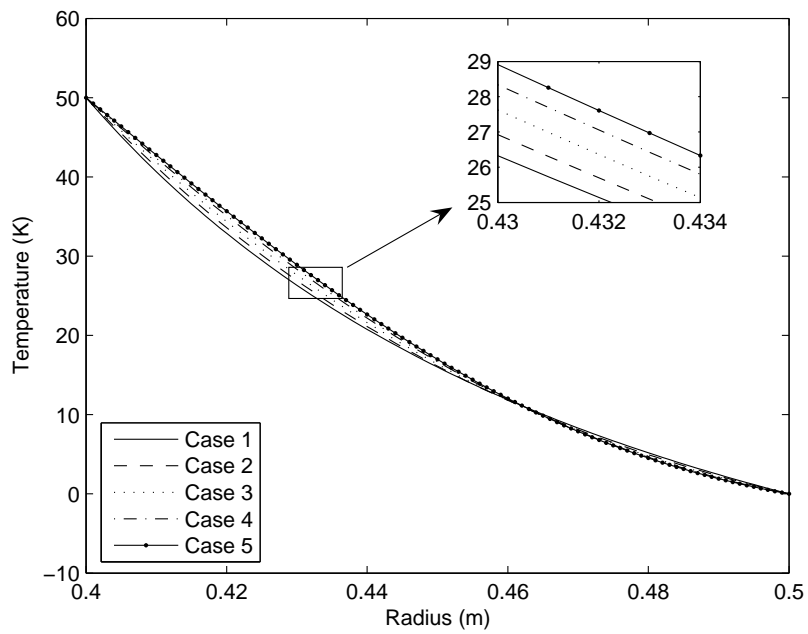


Figure 6 Temperature distribution.

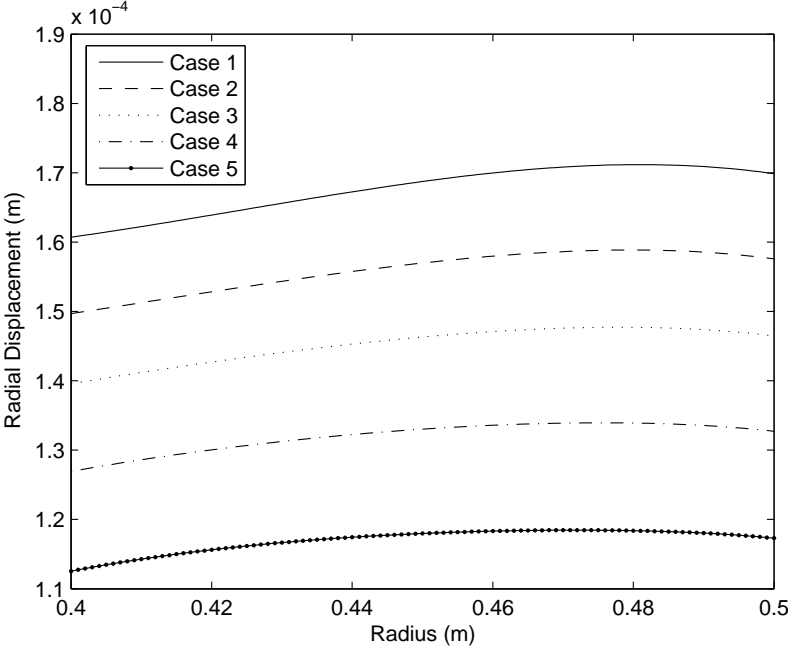


Figure 7 Thermal radial displacement.

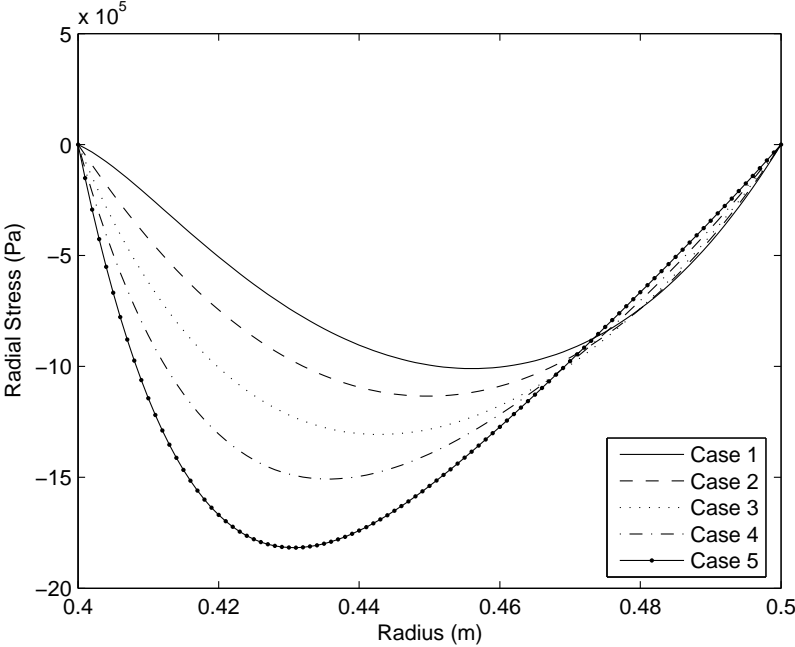


Figure 8 Radial thermal stress.

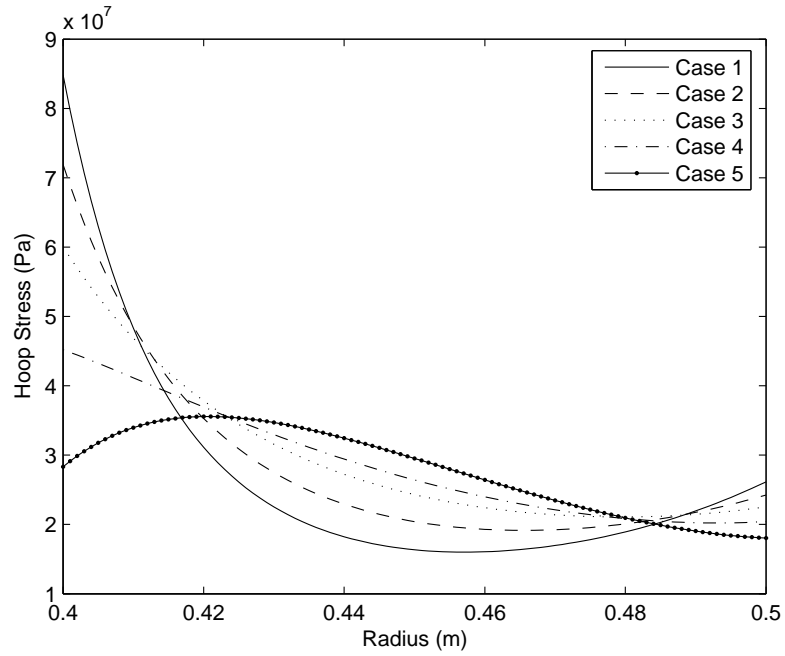


Figure 9 Hoop thermal stress.

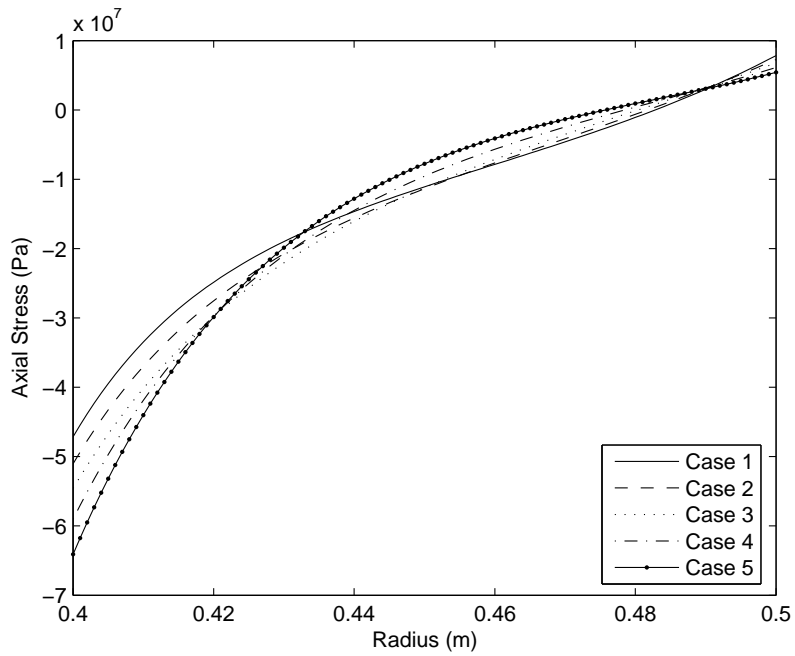


Figure 10 Axial thermal stress.

percent of the metal constituent material in FGM, the radial displacements are increased. Figure (8) represents the radial stress, which satisfies the traction free boundary conditions. The radial stress is zero at the inside and outside boundaries, due to the assumed boundary conditions. Figure (9) shows the hoop stress versus the radial direction. It is observed that the hoop stress variations along the radial direction is lower in metal rich FGMs. As seen, the mechanical hoop stress distribution is compressive at the inside surface and tensile at the outer surface. The axial stress distribution across the cylinder thickness is shown in Fig. (10).

As a second example, a thick circular cylinder under mechanical stresses is considered. The inside and outside pressures are assumed to be 100 MPa and zero, respectively. Figure (11) shows the resulting radial displacements due to the given mechanical boundary condition for different profiles of functionally graded materials. The radial displacements are higher in metal rich functionally graded cylinders. The radial stress along the cylinder thickness is shown in Fig. (12). As seen, the radial stress decreases as the metal density of FGM cylinder decreases. Figure (13) shows the mechanical hoop stress versus the radial direction. It is seen that the hoop stress variations decreases in ceramic rich cases. Finally, the mechanical axial stress versus the radial direction is plotted in Fig. (14). The stress variation across the thickness decreases when the percent of ceramic material constituent increases.

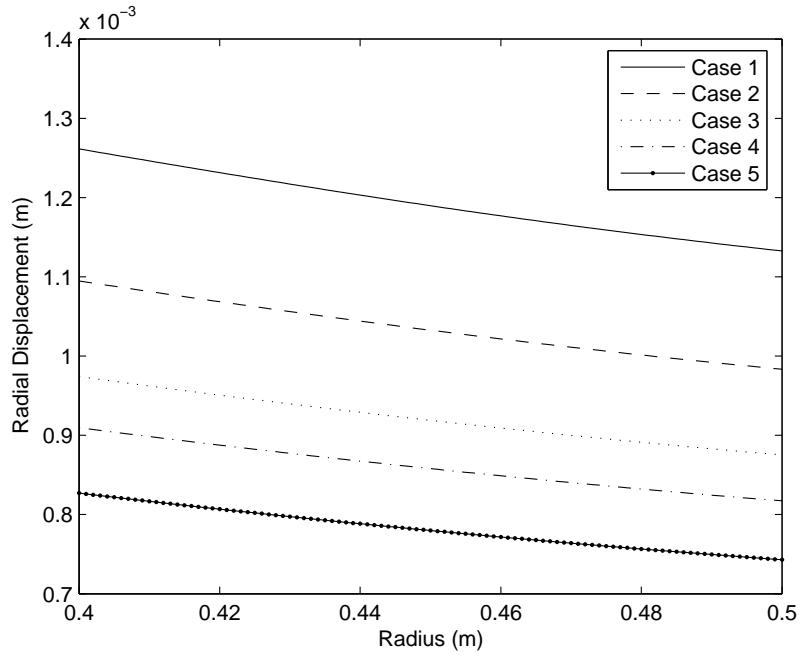


Figure 11 Mechanical radial displacement.

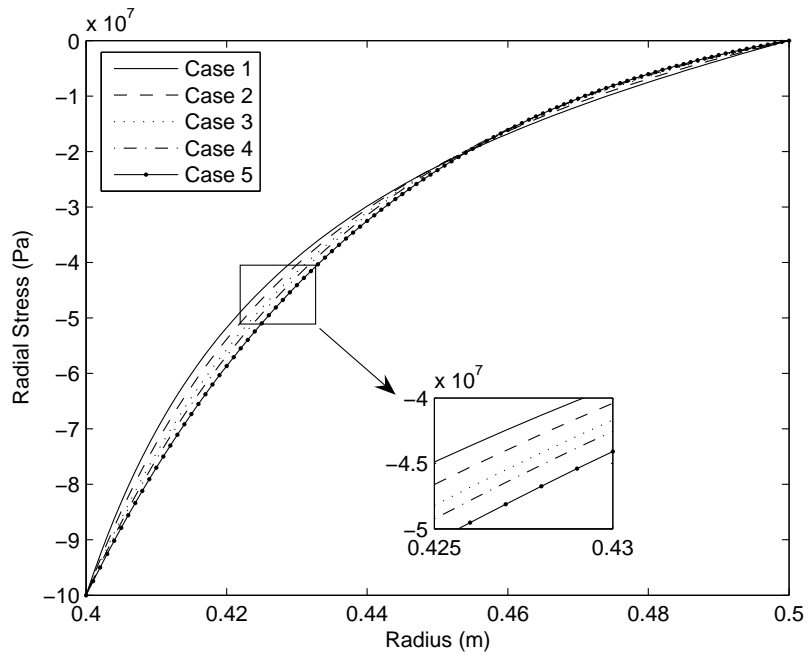


Figure 12 Radial mechanical stress.

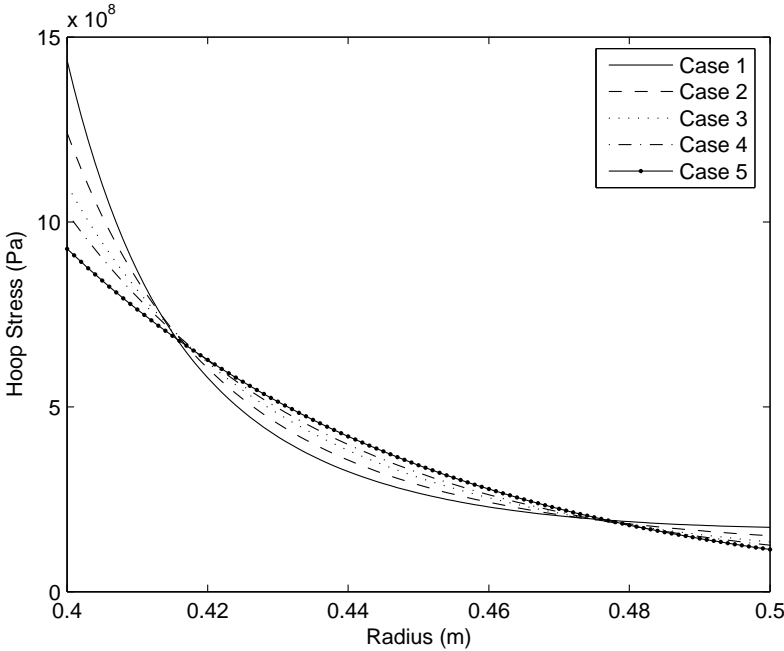


Figure 13 Hoop mechanical stress.

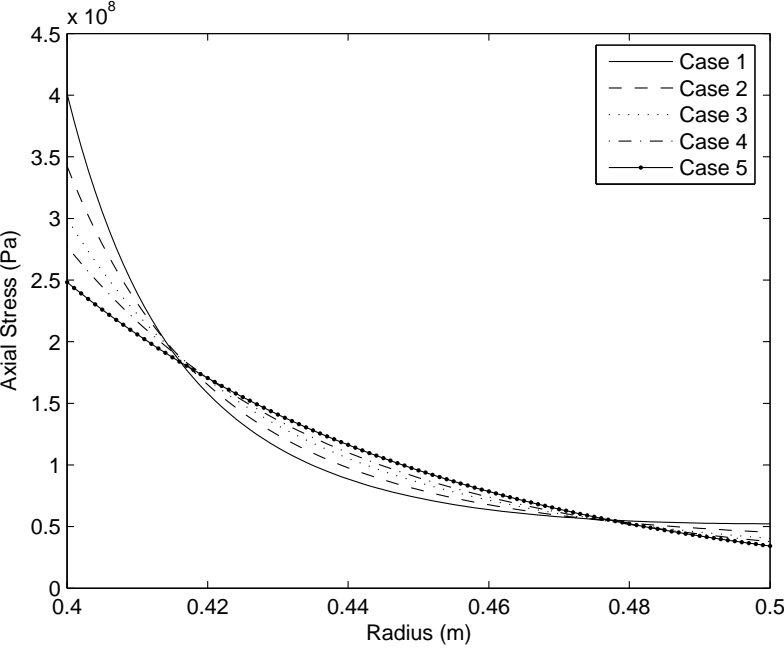


Figure 14 Axial mechanical stress.

6 Conclusions

An analytical solution for the one-dimensional thermal and mechanical stresses in a hollow circular cylinder made of functionally graded material is developed. The constitutive law of functionally graded material is assumed to be of exponential type in radial direction with three constants. These constants allow different variation profiles for the FGM thick cylinder along the radial direction with fixed material boundary conditions at the inside and outside surfaces. Solving the heat conduction and the Navier equations provide the mechanical and thermal stresses.

It is concluded that:

1 - The ceramic rich functionally graded cylinders under the thermal or mechanical loads tend to have lower radial displacement and circumferential stress compared to the metal rich FGM cylinders.

2 - Under the thermal loading, lower circumferential stress is produced in ceramic rich functionally graded cylinders.

3 - Behavior of the axial stress is different for the thermal and mechanical loading conditions. Considering the thermal boundary conditions, the axial stress increases in ceramic FGMs. Vice versa, under the mechanical loading the axial stress for ceramic rich cases decrease.

References

- [1] Obata, Y., and Noda, N., "Steady Thermal Stress in a Hollow Circular Cylinder and a Hollow Sphere of a Functionally Graded Materials", *J. Thermal Stresses*, Vol. 14, pp. 471-487, 1994.
- [2] Ootao, Y., Akai, T., and Tanigawa, Y., "Three-dimensional Transient Thermal Stress Analysis of a Nonhomogeneous Hollow Circular Cylinder Due to a Moving Heat Source in the Axial Direction", *J. Thermal Stresses*, Vol. 18, pp. 497-512, 1995.
- [3] Tanigawa, Y., Morishita, H., and Ogaki, S., "Derivation of System of Fundamental Equations for a Three-dimensional Thermoelastic Field with Nonhomogeneous Material Properties and its Application to a Semi-infinite Body", *J. Thermal Stresses*, Vol. 22, pp. 689-711, 1999.
- [4] Jabbari, M., Sohrabpour, S., and Eslami, M.R., "Mechanical and Thermal Stresses in Functionally Graded Hollow Cylinder Due to Radially Symmetric Loads", *Int. J. Pressure Vessels and Piping*, Vol. 79, pp. 493-497, 2002.
- [5] Jabbari, M., Sohrabpour, S., and Eslami, M.R., "General Solution for Mechanical and Thermal Stresses in a Functionally Graded Hollow Cylinder Due to Nonaxisymmetric Steady-state Loads", *ASME J. Applied Mech.*, Vol. 70, pp. 111-118, 2003.
- [6] Lutz, M.P., and Zimmerman, R.W., "Thermal Stresses and Effective Thermal Expansion Coefficient of a Functionally Graded Sphere", *J. Thermal Stresses*, Vol. 19, pp. 39-54, 1996.
- [7] Zimmerman, R.W., and Lutz, M.P., "Thermal Stress and Effective Thermal Expansion in a Uniformly Heated Functionally Graded Cylinder", *J. Thermal Stresses*, Vol. 22, pp. 177-188, 1999.
- [8] Shao, Z.S., and Wang, T.J., "Three-dimensional Solutions for the Stress Fields in Functionally Graded Cylindrical Panel with Finite Length and Subjected to Thermal/mechanical Loads", *Int. J. Solids Structures*, Vol. 43, pp. 3856-3874, 2006.
- [9] Yee, K.C., and Moon, T.J., "Plane Thermal Stress Analysis of an Orthotropic Cylinder Subjected to an Arbitrary, Transient, Asymmetric Temperature Distribution", *ASME J. Applied Mech.*, Vol. 69(5), pp. 632-640, 2002.
- [10] Tarn, J.Q., "Stress Singularity in an Elastic Cylinder of Cylindrically Anisotropic Materials", *J. Elast.*, Vol. 69(1-3), pp. 1-13, 2002.
- [11] Eslami, M.R., Babaei, M.H., and Poultangari, R., "Thermal and Mechanical Stresses in a Functionally Graded Thick Sphere", *Int. J. Pressure Vessel Piping*, Vol. 82, pp. 522-527, 2005.
- [12] Poultangari, R., Jabbari, M., and Eslami, M.R., "Functionally Graded Hollow Spheres under Non-axisymmetric Thermo-mechanical Loads", *Int. J. Pressure Vessel Piping*, Vol. 85, pp. 295-305, 2008.

- [13] You, L.H., Zhang, J.J., and You, X.Y., "Elastic Analysis of Internally Pressurized Thick Wall Spherical Pressure Vessels of Functionally Graded Materials", *Int. J. Pressure Vessel Piping*, Vol. 82, pp. 347-354, 2005.
- [14] Tutuncu, N., "Stresses in Thick Walled FGM Cylinders with Exponentially-varying Properties", *Engineering Structures*, Vol. 29, pp. 2032-2035, 2007.
- [15] Reddy, J.N., and Chin, C.D., "Thermomechanical Analysis of Functionally Graded Cylinders and Plates", *J. Thermal Stresses*, Vol. 21, pp. 593-626, 1998.
- [16] Rice, R.G., and Do, D.D., *Applied Mathematics and Modeling for Chemical Engineering*, John Wiley and Sons Inc, New York, 1995.
- [17] Hetnarski, R.B., and Eslami, M.R., *Thermal Stresses - Advanced Theory and Applications*, Springer, New York, 2009.

Nomenclature

a, b = Inside and outside radii
 E = Modulus of elasticity
 k = Conductivity
 T = Absolute temperature
 u = Radial displacement
 α = Coefficient of thermal expansion
 ν = Poisson's ratio
 σ_{ij} = Stress tensor
 ϵ_{ij} = Strain tensor

Appendix I) Generalized Bessel Equation

The Bessel differential equation in general form may be considered as [15]

$$x^2 \frac{d^2 y}{dx^2} + x(a + 2bx^r) \frac{dy}{dx} + [c + dx^{2s} - b(1 - a - r)x^r + b^2 x^{2r}]y = 0 \quad (29)$$

where x and y are the independent and dependent variables, respectively, and $a, b, c, d, r,$ and s are some real constants. The solution of the above differential equation depends on the magnitude of the employed constants and coefficients, and may be in form of Bessel functions. If $Z_{\pm p}$ is considered to be a Bessel function, then the general solution of Eq. (29) can be written as

$$y = x^{\left(\frac{1-a}{2}\right)} e^{\left(-\frac{bx^r}{r}\right)} \left[AZ_p \left(\frac{\sqrt{|d|}}{s} x^s \right) + BZ_{-p} \left(\frac{\sqrt{|d|}}{s} x^s \right) \right] \quad (30)$$

where

$$p = \frac{1}{s} \sqrt{\left(\frac{1-a}{2}\right)^2 - c} \quad (31)$$

Depending on the values of $\frac{\sqrt{d}}{s}$ and p , the function Z given in Eq. (30) can be different kinds of Bessel functions as discussed below:

1. If $\frac{\sqrt{d}}{s}$ is real and p is not integer (or zero), then Z_p denotes J_p and Z_{-p} denotes J_{-p} , where J_p is symbol of the Bessel function of the first kind of order p .

2. If $\frac{\sqrt{d}}{s}$ is real and p is integer k (or zero), then Z_p denotes J_k and Z_{-p} denotes Y_k , where Y_k is symbol of the Bessel function of the second kind of order k .

3. If $\frac{\sqrt{d}}{s}$ is imaginary and p is not integer (or zero), then Z_p denotes I_p and Z_{-p} denotes I_{-p} , where I_p is symbol of the modified Bessel function of the first kind of order p .

4. If $\frac{\sqrt{d}}{s}$ is imaginary and p is integer k (or zero), then Z_p denotes I_k and Z_{-p} denotes K_k , where K_k is symbol of the modified Bessel function of the second kind of order k .

Appendix II

Consider a differential equation of the form

$$r^2 u''(r) + r(\lambda r^{\theta_1} - \gamma_1 + 1)u'(r) + \left[\frac{\nu}{1-\nu} \lambda_1 r^{\theta_1} - \frac{\nu}{1-\nu} \gamma_1 - 1 \right] u(r) = 0 \quad (32)$$

where r is an independent variable and u is a dependent one. Also, ν , λ , γ_1 , and θ_1 are some arbitrary constants. Using the general Bessel differential equation [15], the solution of Eq. (32) is

$$\bar{u}(r) = r^{q_1} e^{-\zeta_1 r^{\theta_1}} [AI_p(\zeta_1 r^{\theta_1}) + BI_{-p}(\zeta_1 r^{\theta_1})] \quad (33)$$

Substituting Eq. (33) into Eq. (32), we obtain

$$\left\{ \lambda_1 \left[\frac{\gamma_1 - \theta_1}{2} + \frac{\nu}{1-\nu} \right] r^{\theta_1} + p^2 \theta_1^2 + q_1(q_1 - \gamma_1) - \frac{\nu}{1-\nu} \gamma_1 - 1 \right\} \times [AI_p(\zeta_1 r^{\theta_1}) + BI_{-p}(\zeta_1 r^{\theta_1})] + (2q_1 - \gamma_1)r [AI'_p(\zeta_1 r^{\theta_1}) + BI'_{-p}(\zeta_1 r^{\theta_1})] = 0 \quad (34)$$

For Eq. (34) to be identically satisfied, the coefficients of the equation must be set equal to zero. Setting the coefficients of r^{θ_1} , $[AI'_p(\zeta_1 r^{\theta_1}) + BI'_{-p}(\zeta_1 r^{\theta_1})]$, and $[AI_p(\zeta_1 r^{\theta_1}) + BI_{-p}(\zeta_1 r^{\theta_1})]$ equal to zero, we obtain the following expressions for q_1 , ζ_1 , p , and γ_1

$$\begin{aligned} q_1 &= \frac{\gamma_1}{2} \\ \zeta_1 &= \frac{\lambda_1}{2\theta_1} \\ p &= \frac{1}{\theta_1} \left(\left(\frac{\gamma_1}{2} \right)^2 + \frac{\nu}{1-\nu} \gamma_1 + 1 \right)^{\frac{1}{2}} \\ \gamma_1 &= \theta_1 - \frac{2\nu}{1-\nu} \end{aligned} \quad (35)$$

چکیده

در این مقاله حل تحلیلی تنش های حرارتی - مکانیکی در یک استوانه جدار ضخیم ساخته شده از مواد تابعی تحت شرایط متقارن محوری ارائه شده است. خواص مواد در جهت شعاعی با یک تابع نمائی با سه متغیر تغییر می کند. توابع خطی، توانی و نمائی که معمولاً برای بیان تغییرات خواص ماده در سازه های تابعی مورد استفاده قرار می گیرند دارای دو ثابت می باشند که با توجه به ارضاء خواص ماده تابعی در شعاع داخل و خارج دو ثابت آنها مشخص شده و نهایتاً پروفیل تغییرات ماده بین سطح داخل و خارج ثابت می ماند. تابع پیشنهادی در این مقاله دارای سه ثابت می باشد که با ارضاء خواص ماده در سطوح داخل و خارج یک ثابت اضافی در اختیار می گذارد که می توان پروفیل تغییرات مواد تابعی را در بین سطح داخل و خارج انتخاب نمود. با استفاده از این تابع با سه ثابت حل تحلیلی مسئله با استفاده از توابع بل و متد لاگرانژ و با استفاده از معادلات ناویر بدست آورده شده است.